Moose Habitat Selection and Movement Dynamics in a Changing Thermal Landscape under Climate Change

Accounting for circadian rhythmicity using harmonic terms

Niels van der Vegt

Independent project • 30 credits
Swedish University of Agricultural Sciences, SLU
Department of Wildlife, Fish, and Environmental Studies
Examensarbete / SLU, Institutionen för vilt, fisk och miljö
2024:5
Umeå, 2024

Moose Habitat Selection and Movement Dynamics in a Changing Thermal Landscape under Climate Change - Accounting for circadian rhythms using harmonic terms

Niels van der Vegt

Supervisor:	Wiebke Neumann, Swedish University of Agricultural Sciences, Department of Wildlife, Fish, and Environmental Studies
Assistant supervisor:	Sytze de Bruin, Wageningen Universty, Department of Geo-information Sciences
Examiner:	Tim Hofmeester, Swedish University of Agricultural Sciences, Department of Wildlife, Fish, and Environmental Studies

Credits:	30 credits
Level:	A2E
Course title:	Master’s thesis in Biology
Course code:	EX0971
Course coordinating dept:	Department of Wildlife, Fish and Environmental Studies
Place of publication:	Umeå
Year of publication:	2024
Title of series:	Examensarbete / SLU, Institutionen för vilt, fisk och miljö
Part number:	2024:5

Keywords:
Heatwaves, Moose, Habitat selection, Behavioral thermoregulation, Step Selection Functions

Swedish University of Agricultural Sciences
Faculty of Forest Sciences
Department of Wildlife, Fish, and Environmental Studies

Abstract

Keywords: Heatwaves, Moose, Habitat selection, Behavioral thermoregulation, Step Selection Functions

Climate change is intensifying the frequency and severity of heatwaves in boreal regions, posing challenges for heat-sensitive species like the moose (*Alces alces*). As a large-bodied herbivore with limited heat tolerance, the moose is especially vulnerable to rising temperatures.

This thesis examined fine-scale movement and habitat selection of 300 GPS-collared female moose across four ecological strata in Sweden during heatwaves. Time-varying Step Selection Functions and space-time regression kriging were used to analyze behavioral responses to thermal stress.

Moose reduced daytime movement during heatwaves, suggesting behavioral thermoregulation. Habitat selection shifted in some regions, with increased use of forest and wetland habitats during midday, indicating preference for thermal refuges. Moose also selected lower elevations in certain strata, likely to access cooler microclimates, while proximity to water did not consistently influence selection and was avoided in open alpine wetlands.

These findings reveal that moose employ spatial strategies to cope with heat, emphasizing the importance of landscape features in buffering thermal extremes. Such insights are crucial for anticipating climate impacts and guiding wildlife management in a warming world.

Table of contents

List of tables

List of figures

Abbreviations

Abbreviation	**Description**
API	Application Programming Interface
DEM	Digital Elevation Model
EPSG	European Petroleum Survey Group (coordinate reference system code)
GIRS	Geo-information Science and Remote Sensing
GPS	Global Positioning System
GTT	Geometric Temperature Trend
HMM	Hidden Markov Model
LiDAR	Light Detection and Ranging
NDVI	Normalized Difference Vegetation Index
QGIS	Quantum Geographic Information System
RSF	Resource Selection Function
SQL	Structured Query Language
SSF	Step Selection Function
SWEREF-99	Swedish Reference Frame 1999
TRI	Terrain Ruggedness Index
WRAM	Wireless Remote Animal Monitoring

1. Introduction

Climate change is increasing the frequency and intensity of heatwaves, even in traditionally cooler northern regions. Large herbivores are increasingly challenged by rising ambient temperatures, which can constrain their activity patterns, alter resource use, and compromise fitness. As climate change intensifies, understanding how these species behaviorally buffer thermal stress is essential for predicting their resilience and guiding conservation efforts (Hetem et al. 2014; Felton et al. 2024). Extreme heat events pose a significant challenge for moose (*Alces alces*), a species adapted to cold climates but ill-equipped to dissipate excess heat (Renecker & Hudson 1989). Moose have a highly insulative coat, thick skin, and a low surface-area-to-volume ratio, all of which minimize heat loss and were advantageous in their evolutionary past (Niedziałkowska et al. 2022). However, these same adaptations become liabilities in hot weather, making moose prone to heat stress at relatively low ambient temperatures. Historically research has noted that moose can begin experiencing signs of thermal stress when temperatures rise above approximately 14 °C (Renecker & Hudson 1989). However, recent physiological studies challenge this simplification. Thompson et al. (2020) monitored free-ranging moose and found no single ambient temperature at which heat stress reliably occurred. Instead, stress indicators and body temperature varied dynamically with prior-day conditions such as solar radiation and humidity. Unlike many large mammals, moose lack the effective sweat glands necessary for evaporative cooling and instead rely on panting and other behaviors to shed heat (Renecker & Hudson 1989; Verzuh et al. 2023a). In effect, a moose's physiology provides limited options for cooling, meaning behavioral adjustments are critical for avoiding hyperthermia.

Moose typically exhibit a bimodal activity pattern, with distinct peaks at dawn and dusk corresponding to crepuscular foraging behavior (Neumann et al. 2012). When faced with heat stress, they increase their movement during twilight and night (Montgomery et al. 2019). In addition, moose mitigate heat by actively seeking cooler microhabitats. For example, they bed in deep shade (dense conifer stands or wooded bogs) when air temperature rises, effectively raising their thermal tolerance (McCann et al. 2013).

This thermoregulatory behavior comes at the cost of missing daytime foraging opportunities. Prolonged heatwaves can curtail feeding opportunities and lead to reduced energy intake. If moose spend significantly less time eating during summer due to heat avoidance, they may gain less body mass and enter winter in poorer condition. In fact, moose that cease foraging during hot weather risk insufficient fat reserves by autumn, with cascading impacts on reproduction and survival (van Beest & Milner 2013). Body fat plays a critical role in moose reproduction, as individuals with at least 2 mm of rump fat have a high likelihood of being pregnant in midwinter, and greater fat reserves are associated with increased chances of calf production and survival (Monteith et al. 2015). Consistent with this, unusually warm summers have been linked to poor body condition and even population declines at the southern extent of the moose's range, where individuals cannot easily find thermal refuge (Lenarz et al. 2009). Taken together, the evidence suggests that moose rely on a suite of avoidance behaviors to survive high temperatures, but those same behaviors may negatively affect individual fitness and population dynamics as climates continue to warm. Beyond individual physiology and behavior, it is important to recognize that moose occupy a keystone role in boreal ecosystems. As large herbivores, moose function as ecosystem engineers that influence their environment. Their feeding habits can shape forest composition and carbon storage, for instance, intense moose browsing in summer can substantially reduce new woody growth and even alter regional carbon balance (Persson et al. 2005). By preferentially feeding on certain trees and shrubs, moose regulate forest structure and plant community dynamics over large areas. This in turn affects habitat conditions for other species and ecological processes like nutrient cycling. Moose browsing and the deposition of urine and feces redistribute nutrients from plants into the soil, thereby accelerating below-ground nitrogen cycling in heavily used areas (Bump et al. 2017). If climate-driven heat stress causes moose to alter their habitat use or daily activity there may be broader ecological consequences. Understanding moose thermal behavior is therefore not only about the animals themselves but also about anticipating shifts in ecosystem functioning under climate change.

To date, most studies of moose thermoregulatory behavior using telemetry have taken place in the southern parts of the species' range or in more temperate settings, often under conditions where there is a clear day-night cycle (Lenarz et al. 2009; van Beest et al. 2012; Montgomery et al. 2019). Fewer studies have focused on moose in the far north, where climate warming is occurring rapidly and photoperiod extremes are the norm (Jennewein et al. 2020). Additionally, previous research has often relied on binning the temporal dimension into discrete times of the day (e.g. dawn, dusk, day night) (van Beest et al. 2012). Temperature covariates have also been summarized as daily maximums, an approach that may miss fine-scale spikes in temperature and the immediate behavioral adjustments moose make hour by hour (Lenarz et al. 2009). While such studies have provided valuable insights, they lack the temporal detail to analyze how moose behavior changes within a single hot day or over the course of a multi-day heatwave. Moreover, past analyses often did not explicitly isolate heatwave events but rather correlated temperatures with moose behaviors. This leaves a knowledge gap in understanding the acute, context-specific behavioral shifts that occur during heatwaves, as opposed to the baseline summer behavior under milder conditions. To our knowledge, no prior study has simultaneously examined moose activity patterns with high temporal detail and in relation to discrete heatwave events, particularly while accounting for circadian context across different photoperiod regimes.

Studying moose responses to heat in high-latitude environments brings additional complexity due to extreme photoperiods. At latitudes above the Arctic Circle, summers are characterized by the midnight sun, a period of continuous or near-continuous daylight. The absence of a regular light-dark cycle can disrupt normal circadian rhythms that many animals rely on to time their behavior. Under typical conditions, daily patterns of activity and rest are synchronized to daylight and darkness by an internal circadian clock. In Arctic summers, however, those external cues are weak or absent for weeks on end. Prior research on other northern ungulates has shown that continuous summer daylight can diminish 24-hour activity cycles. Instead animals may adopt an arrhythmic or free-running activity pattern when day and night become indistinguishable (van Oort et al. 2005). For example, wild reindeer (*Rangifer tarandus*) living at ~79° N latitude showed a loss of their normal daily activity rhythm during periods of perpetual sunlight (van Oort et al. 2005). Moose in subarctic and arctic regions might likewise break away from circadian behavioral rhythms during the midnight sun. Instead of the pronounced diurnal cycle seen in lower latitude, high-latitude moose could exhibit more irregular patterns. On the other hand, some studies suggest certain physiological rhythms (e.g. the hormone melatonin) persist despite continuous light, indicating that internal clocks are not entirely lost even in polar environments (Stokkan et al. 2007). Investigating moose behavior across a latitudinal gradient, from regions with a pronounced day-night cycle to those with midnight sun, can shed light on how heat stress responses influence circadian processes.

1.1 Objectives and Hypotheses

In this thesis, I address the above knowledge gaps by analyzing fine-scale moose movement and habitat selection during documented heatwaves across a range of environmental contexts. My goal is to determine how moose modify their behavior in response to short-term extreme heat, and whether these modifications vary with respect to ecotype and latitude. Focus is laid on incorporating the temporal context of thermoregulatory behavior. By interpolating environmental data on similarly fine timescales, I perform a context-aware analysis of moose behavior during heatwaves. Ultimately, this approach allows me to test whether moose exhibit the expected heat-avoidance behaviors at a fine temporal scale and to explore how the daily rhythmicity of moose behavior is maintained or altered under the combination of heat stress and extreme daylength. I hypothesize the following:

I Heat-Avoidance Behavior Hypothesis**:** During heatwave conditions, moose will exhibit pronounced heat-avoidance behaviors consistent with prior observations of heat-stressed moose. Specifically, they are expected to reduce movement during the hottest hours and increase use of shaded or thermally buffered habitats such as dense forest and wetland areas.

II Circadian Rhythm Modulation Hypothesis**:** Daily activity patterns will be modulated by both heat stress and latitude. Moose in regions with continuous or prolonged daylight (> 63 °N) are expected to show weaker circadian rhythmicity, and during heatwaves, activity will shift toward cooler hours, regardless of light cues. This latter pattern is anticipated to be more pronounced in boreal than in temperate populations.

III Foraging Opportunity Hypothesis**:** Moose will attempt to offset reduced daytime foraging by intensifying selection for high-quality foraging habitats (e.g. clear-cut and young forest) during cooler periods of the heatwave cycle, such as evening or early morning hours.

IV Water-Seeking Behavior Hypothesis**:** During heatwave events, moose will exhibit increased selection for proximity to water sources to aid in thermoregulation through direct contact.

V Topographic Refuge Hypothesis: In mountainous or alpine regions, moose will shift their location toward higher elevations during heatwaves in search of cooler air temperatures. This upslope movement is expected to be most evident during midday hours when thermal stress peaks.

2. Theoretical Framework

2.1 Step Selection Functions (SSF)

With the increasing availability of telemetry data, new approaches have emerged to model habitat selection and movement decisions. Step selection functions (SSFs) provide a framework for understanding fine-scale movement choices of individual animals by analyzing them on a step-by-step basis (Lenarz et al., 2009). A step represents a movement decision, and it is defined as the straight-line segment between two consecutive recorded locations of an individual. SSFs compare observed steps to alternative steps the animal could have taken, but did not, thereby allowing selection to be evaluated relative to availability (Mawer et al. 2023). Each observed step is paired with a set of alternative steps drawn from an empirical movement distribution fitted to the animal's movement patterns. Commonly used distributions are a (zero-inflated) Gamma distribution for step length, and a von Mises distribution for turning angle (Signer et al. 2019; Fieberg et al. 2021). The probability of selecting a particular step is estimated based on covariates associated with each step. To model habitat preferences and accessibility, environmental covariates such as vegetation type or elevation can be included. Similarly step length, log-transformed step length, and turning angle can be included to account for an animal's movement tendencies. Finally, interactions of environmental and movement covariates can be included at the start of the step to model how directly and quickly an animal can move through the landscape (Signer et al. 2019).

The general form of an SSF resembles a resource selection function (RSF) and is expressed in exponential form as (Eq. 1):

$$\omega(x_i) = \exp(\beta_1 x_{i1} + \beta_2 x_{i2} + \cdots + \beta_n x_{in}) \tag{1}$$

Where x_i denotes the step and associated covariates of the i-th step in a set of m candidate steps, and x_{i1} to x_{in} represent the individual covariates describing that step. The function ω returns the relative weight assigned to the step based on its covariates. This value reflects how likely a step is to be chosen relative to other candidate steps, but is not itself a probability. To compute the conditional probability of selecting a specific step x_i from a set of m available steps the relative weights are normalized across all candidates. This gives the probability of selecting step i, conditional on the set of m available steps (Eq. 2):

$$P(x_i) = \frac{\omega(x_i)}{\sum_{j=1}^{m} \omega(x_j)} = \frac{\exp(\beta_1 x_{i1} + \beta_2 x_{i2} + \cdots + \beta_n x_{in})}{\sum_{j=1}^{m} exp(\beta_1 x_{j1} + \beta_2 x_{j2} + \cdots + \beta_n x_{jn})} \quad (2)$$

The coefficients β_1 to β_n are estimated using conditional logistic regression, which maximizes the likelihood of observed steps relative to available steps. After model fitting, the exponentiated coefficients β indicate the relative selection strength for each covariate and are interpreted differently depending on whether the covariate is continuous or categorical. For continuous covariates, the coefficient β represents the change in the relative probability of step selection associated with a one-unit increase in the covariate, holding other variables constant. A coefficient of $\beta > 0$ indicates that for each one-unit increase in the covariate, the step becomes more likely to be selected. Conversely, a coefficient of $\beta < 0$ indicates that for each one-unit increase in the covariate, the step becomes less likely to be selected. For categorical covariates, the interpretation of the coefficient is relative to a reference category. If $\beta > 0$, steps that fall into that category are more likely to be selected relative to the reference category. If $\beta < 0$, steps in that category are less likely to be selected compared to the reference category.

2.2 Accounting for Circadian Rythms using Harmonic Terms

Recent studies on SSFs have increasingly emphasized the importance of incorporating behavioral states as explanatory variables for movement decisions (Chatterjee et al. 2024; Klappstein et al. 2024). An animal's behavioral state strongly influences its needs and movement characteristics during a step. Accounting for behavior can be done by including behavioral state as an interaction term with environmental and movement covariates and by fitting movement distributions to movement data associated with each behavioral state (Chatterjee et al. 2024).

Predicting an animal's behavior based on movement metrics is commonly done using state-predicting models such as Hidden Markov Models (HMMs). HMMs classify each movement step into discrete states (e.g., foraging vs. resting), generally based on movement metrics, through clustering techniques (McClintock & Michelot 2018). However, this approach has limitations depending on the temporal resolution of the data. At large enough time intervals, animals may switch between behavioral states multiple times between successive GPS fixes. In such cases, HMMs can only provide a coarse approximation of true behavioral dynamics, potentially oversimplifying behavior during the interval or failing to capture a behavioral shift accurately (Langrock 2016). An alternative approach that avoids this, is to use time-of-day categories, such as day, night, crepuscule, or other zeitgebers that cue circadian behavior (van Beest et al. 2012). However, in high-latitude environments, such as our moose localizations within the Arctic Circle, the absence of night and crepuscular periods during the summer polar sun renders traditional time-of-day categorizations ineffective.

A more flexible approach compared to discrete behavior, or time-of-day categories would be through incorporating cyclical terms to represent changes over a diel. If we consider that selection for a covariate will most likely have some periodic function associated with an animal's circadian rhythm, we can model this as a Fourier series of trigonometric functions. These harmonic terms, based on a Fourier series, allow coefficients to vary cyclically over a 24-hour period. This transforms the step selection function into a time-varying model, which predicts step probability based on covariates, into a dynamic harmonic regression that incorporates variability during a day. The method from Forrest et al. (2025) is incorporated, extending the SSF by incorporating harmonic terms as interaction effects with our main covariates (Eq. 3.1):

$$\omega\big(x_i, \beta_t(\tau;\alpha)\big) = \exp(\beta_1(\tau;\alpha_1)x_1 + \cdots + \beta_n(\tau;\alpha_n)x_n) \qquad (3.1)$$

In this model x is the step and its associated covariates. $\beta_t(\tau;\alpha)$ returns a time-varying coefficient based on the time of the step τ. The vector $\alpha_i = (\alpha_{i,0}, \dots, \alpha_{i,2P})$ contains coefficients for the trigonometric functions that control how the covariate x_i changes over time. Coefficients are defined for p pairs of harmonics and $\mathrm{B}_t(\tau;\alpha_i)$ is given as (Eq. 3.2):

$$\beta_{ti}(\tau;\alpha) = \alpha_{i,0} + \sum_{j=1}^{P} \alpha_{i,j} \sin\left(\frac{2j\pi\tau}{T}\right) + \sum_{j=1}^{P} \alpha_{i,j+P} \cos\left(\frac{2j\pi\tau}{T}\right) \qquad (3.2)$$

Here, $\alpha_{i,0}$ is the main effect of the covariate, which can be considered the affinity or aversion for a covariate irrespective of circadian rhythm. T represents the period associated with the seasonality, which is a diel in our case. j sets the frequencies of the sine and cosine functions. Increasing the number of harmonic pairs with different values of j allows for finer temporal fluctuations of covariates, but caution is needed to avoid overfitting (Forrest et al. 2025). Alternatively, periodic functions can be modeled using spline functions, as recently shown in (Klappstein et al. 2024). However, this approach requires significantly more computational power and was not explored further in this study.

2.3 Population inference using Step Selection Functions

When estimating population-level effects from individual tracked animals, it is important to account for behavioral differences among individuals and within-individual correlation in habitat use due to spatial auto-correlation (Fieberg et al. 2010; Chatterjee et al. 2024). Ignoring these factors violates the assumption of independence, leading to overfitted models and underestimated uncertainty (Fieberg et al. 2010; Muff et al. 2020).

One approach to address this issue is fitting a random-effects model with random slopes, where each individual receives unique slopes for relevant explanatory variables (Klappstein et al. 2024). However, this method is computationally demanding, and the number of parameters increases substantially when incorporating harmonics, due to the many possible combinations of individual-level random slopes and harmonic terms. A simpler alternative is the two-stage conditional logistic regression approach (Fieberg et al. 2010). This method first fits a SSF separately for each individual and then averages the resulting coefficients to infer population-level responses. This approach is effective when sufficient data have been collected to estimate individual regression parameters, and when individuals can be considered independent (Fieberg et al. 2010; Muff et al. 2020). In moose, individual independence is a reasonable assumption despite shared population ranges, as they are largely solitary and exhibit limited social coordination (Niedziałkowska et al., 2022). To summarize population effects, the mean value of the individual coefficients for an explanatory variable can be used. However when estimating variance, this method overestimates as it does not account for the inherent sampling uncertainty in the coefficient estimates of each animal (Fieberg et al. 2010). This uncertainty can be accounted for by weighting of each individual's estimate according to its sampling variance. In practice this can be achieved by estimating the mean using an intercept-only linear regression model with inverse-variance weighting (Eq. 4).

$$\widehat{\beta_{\mathrm{population}}} = \frac{\sum_{i=1}^{n} \frac{\beta_i}{\mathrm{Var}(\beta_i)}}{\sum_{i=1}^{n} \frac{1}{\mathrm{Var}(\beta_i)}} \tag{4}$$

Finally, in the two-stage conditional logistic regression approach, it is important that each value in a categorical variable is visited by each animal at least once (Fieberg et al. 2010; Muff et al. 2020). For instance, each habitat category being investigated should be represented in the data for every individual animal. If this condition is not met, the individual SSF will fail to estimate the selection for the missing category. While random effects models are capable of handling missing categories, concerns should be raised about the interpretability of such estimates, as well as the reliability of the resulting variances.

2.4 Interpolating temperature using Space-Time Regression Kriging

Obtaining temperature at an animal's step location has been approached through multiple methods. The most direct method involves using readings from a temperature sensor attached to the animal's collar, provided this data is available. The key advantage of this approach is that there is no spatial or temporal discrepancy between the recorded temperature and the step location. On average, collar temperature measurements track ambient temperature trends but tend to exhibit consistently higher values, for example due to neck collar exposure to solar radiation (Ericsson et al., 2015; Messeri et al., 2019). Despite this general consistency, outliers are common due to factors such as body heat, sensor irradiation, placement, and air circulation. These factors can lead to overestimations of ambient temperature, sometimes exceeding the daily maximum temperature range (Messeri et al. 2019). An alternative approach is to use temperature data from the nearest weather station. This avoids sensor-related artifacts but introduces spatial and temporal mismatches. Weather stations are distributed unevenly across the landscape, and their reporting frequencies vary. Consequently, the spatial and temporal distances between an animal's step and the nearest available temperature measurement differ between observations, introducing variability in explanatory data. These discrepancies can be mitigated by employing interpolation techniques that integrate both spatial and temporal dimensions to estimate temperature conditions at the precise locations and times of animal movements.

Kriging is a geostatistical interpolation method that provides an estimate of an unknown value at a given location by leveraging spatial autocorrelation in the data (Cressie & Wikle 2011). The fundamental idea is that nearby observations tend to be more similar than distant ones, and this relationship can be modeled using a covariance function. In its simplest form, ordinary kriging estimates an unknown value $\hat{Z}(s_0)$ at spatial location s_0 as a weighted sum of observed values from neighboring locations s_i $(Eq. 5)$:

$$\hat{Z}(s_0) = \sum_{i=1}^{n} \lambda_i \, Z(s_i) \tag{5}$$

where λ_i are kriging weights that determine the contribution of each neighboring observation to the estimate. These weights are derived by solving a system of equations that minimizes prediction variance (Cressie & Wikle 2011), where the semi variance of the difference between observations separated by a distance h is modeled using a semi-variogram $\gamma(h)$.

While ordinary kriging relies solely on spatial autocorrelation, prediction can be improved by incorporating known environmental predictors through regression kriging**.** This approach first models a trend of the variable of interest, such as temperature, as a function of explanatory covariates (e.g., elevation, land cover, or latitude). After factoring out all explanatory factors, remaining spatial patterns are modeled and subsequently addressed using kriging of the residuals (Hengl et al. 2007). The predicted value takes the form of Eq. 6, taken from (Hengl et al. 2007):

$$\hat{Z}(s_0) = \hat{m}(s_0) + \hat{e}(s_0) = \sum_{k=0}^{p} \widehat{\beta_k} \cdot q_k(s_0) + \sum_{i=1}^{n} \lambda_i \cdot e(s_i) \qquad (6)$$

where $\hat{m}(s_0)$ is the trend component of temperature, predicted through regression, $\hat{e}(s_0)$ is the residual component, predicted through kriging. In the regression model, explanatory variables at location s_0 are represented by $q_k(s_0)$ with coefficient β_k. We can further expand this by considering the temporal dimension in our estimates, performing space-time kriging by deriving the kriging system in three dimensions (Eq 7).

$$\hat{Z}(s_0, t_0) = \sum_{i=1}^{n} \lambda_i Z(s_i, t_i) \qquad (7)$$

An in-depth introduction to space-time kriging is out of scope for this study, but the reader is referred to (Montero et al. 2015) for an in-depth look into to the topic.

3. Material and Methods

3.1 Moose Localisations and Strata

Data Pre-processing

Moose location data were obtained from the Wireless Remote Animal Monitoring (WRAM) database, which compiles telemetry data from individual studies conducted since 2003 (Dettki et al. 2013). GPS collars fitted to moose recorded locations at three-hour intervals. The study was restricted to female moose to avoid the irregular movements and behaviors associated with the rutting season in males, and because the majority of available data originated from females. Data from all available years were included but limited to the summer season, defined as June through August, to exclude the migratory periods typical of moose in northern Sweden (Van Moorter et al. 2021). To ensure a representative temporal sample of seasonal temperature, only tracking segments where moose were monitored for at least 70% of the summer season were included. This threshold was calculated by determining the theoretical maximum number of possible fixes within the June–August period (based on three-hour intervals) and dividing the number of actual recorded fixes by this value. Duplicate localizations and those recorded outside the borders of Sweden were removed. To account for ecological differences and regional variation in moose behavior, the study area was divided into strata based on limnic ecosystem data from the Swedish Environmental Protection Agency and the forest-mountain boundary defined by the Swedish Forest Agency (Fig. 2). The forest-mountain boundary was used as it marks the cessation of production forestry activities; beyond this point, clear-cut areas no longer occur, removing an important foraging habitat type that moose heavily utilize in other strata. The resulting strata were classified as Boreal Alpine, Boreal Inland, Boreal Coastal, and Temperate**.** Short-term transitions between strata, where moose briefly moved into a different stratum, were filtered out by retaining only locations from the dominant stratum, determined based on the majority of recorded fixes for each individual. After applying these filters, a total of 400,181 localizations from 300 moose were retained for analysis. Due to the use of data originating from multiple historical studies, the number of localizations varied among strata: Boreal Alpine (44%), Boreal Coastal (14%), Boreal Inland (8%), and Temperate (28%). Figure 1 shows the strata, with moose localizations per year represented as point data.

Random Step Generation

For each observed step, 15 random steps were generated using the `amt` package in R (Signer et al. 2019). Step lengths were modeled using a gamma distribution, and turning angles were modeled using a von Mises distribution, both standard choices for animal movement modelling (Fieberg et al. 2021). Distributions were first fitted separately for each stratum, thereby estimating step-length and turning-angle distributions at the population level, with each stratum treated as a distinct population. This approach was adopted because moose inhabiting the boreal strata exhibit different morphology and movement behaviors compared to those in the temperate stratum, as reflected in their respective fitted step-length distributions. Fitting movement distributions at the population rather than the individual level facilitated the adjustment of the selection-free movement kernel to the actual movement kernel, resulting in gamma and von Mises distribution parameters specific to each stratum (Forrest et al. 2025).

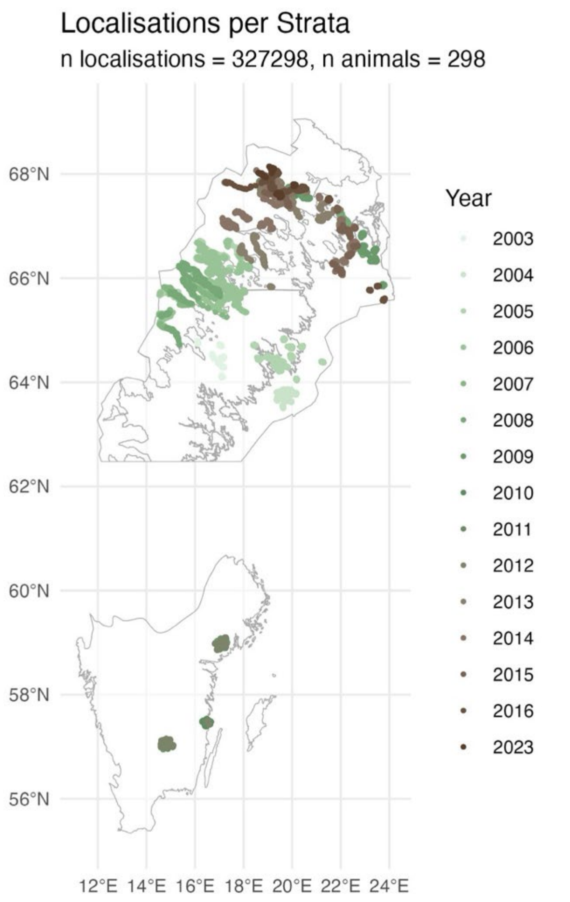

Figure 1: All pre-processed moose localisations. Sweden is divided in four strata for this study, defined by grey lines in this figure. Boreal Alpine (top left), Boreal Inland (top middle), Boreal Coast (top right), and Temperate (south). The localisation's color refers to the year it was obtained.

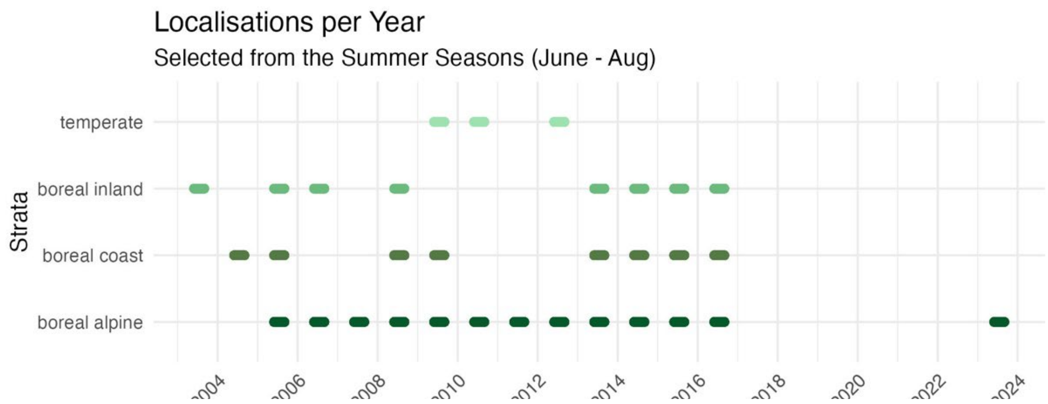

Figure 2: Localisations included within the four strata. Each dash represents a summer of moose localisations within that stratum.

3.2 Sampling Geographical Covariates

Each localization was annotated with a set of geographical covariates hypothesized to influence moose movement behavior during heatwaves. Covariates were selected either because they represented potential points of attraction, such as dense forests and clear-cut areas providing favorable foraging conditions, or potential points of repulsion, such as rugged terrain. An overview of the covariates included in the analysis is provided in Table 1.

Land use data were obtained from the Swedish Environmental Protection Agency's National Land Cover Database (Naturvårdsverket 2003). Two datasets were used: one from 2003 with a spatial resolution of 25 m × 25 m, and one from 2018 onward with a spatial resolution of 10 m × 10 m. Land use categories were simplified into eight classes: coniferous forest, deciduous and mixed forest, clear-cut and young forest, low-mountain forest, wetlands, open areas, water bodies, and anthropogenic land. Because the land use data represented snapshots in time, forestry changes that occurred after the publication dates of these datasets would not be captured, despite the importance of clear-cuts as foraging habitats for moose. To address this, forest felling data from the Swedish Forest Agency were incorporated to manually update the land use maps (Skogsstyrelsen, 2024). Localizations that occurred within ten years after a recorded felling event were reassigned to the "clear-cut and young forest" land use class. The average distribution of land use classes used by moose in each stratum between June and September is shown in Figure 3. Based on these distributions, it was observed that moose predominantly utilized three to four specific habitat types per stratum. Therefore, for each stratum, only these commonly used habitat classes were retained for modeling, while the remaining classes were combined into a single "other" category. This step was necessary to meet the requirements of the two-stage SSF modeling approach, which assumes that each individual animal has visited each habitat class included in the model at least once.

In addition to land use, proximity to water sources was included as a covariate to investigate whether moose preferentially moved closer to water during heatwave conditions. A continuous raster layer of distances to the nearest water source was generated by applying the Proximity (Raster Distance) tool in QGIS to the water bodies layer derived from the land use map. Elevation was also included as an environmental covariate. Elevation data were obtained from Lantmäteriet at a spatial resolution of 50 m × 50 m (Lantmäteriet 2009). From these data, a terrain ruggedness index (TRI) was calculated following the method described by Riley et al. (1999) to quantify topographic heterogeneity, which could influence movement costs and habitat selection.

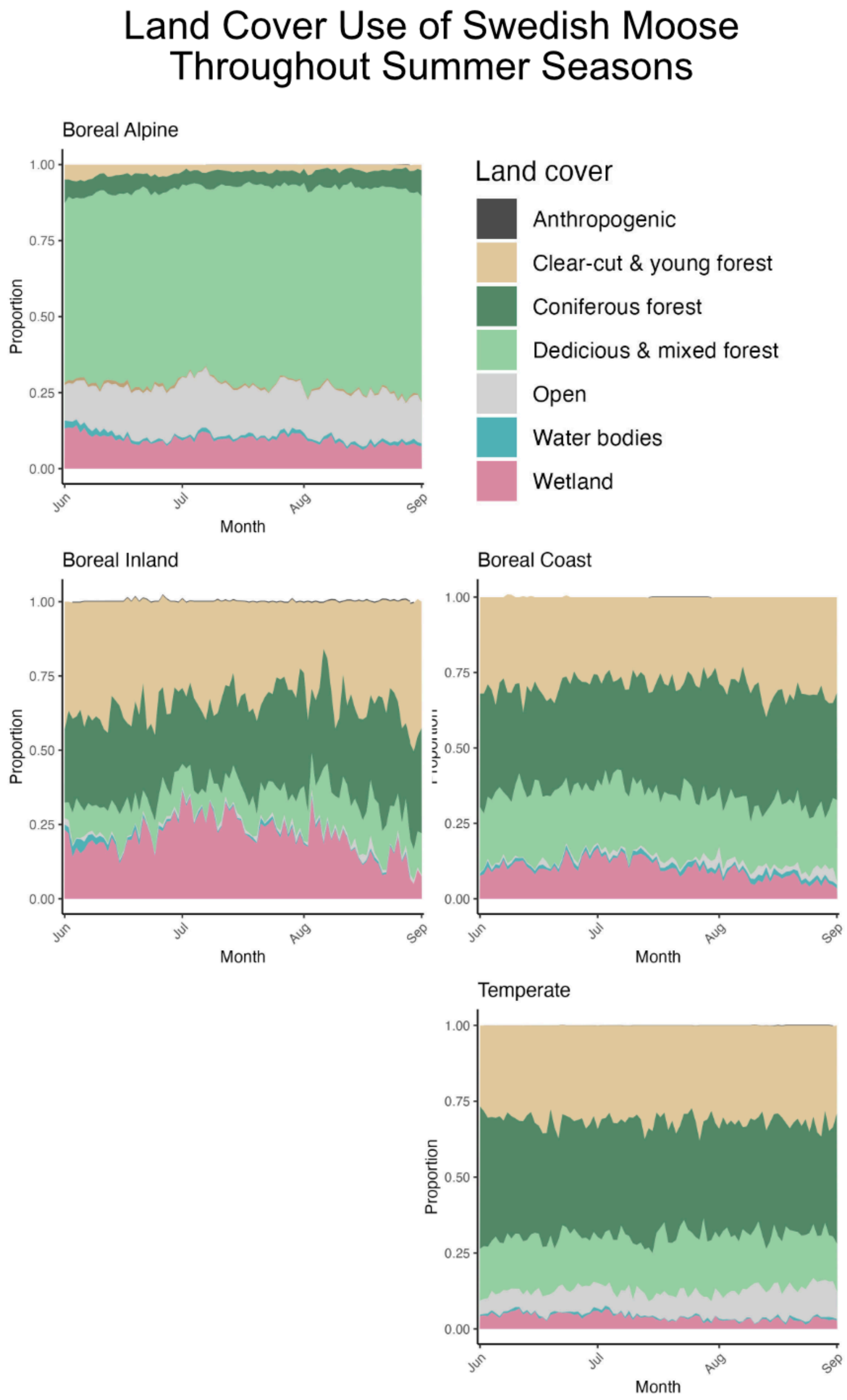

Figure 3 : Proportions of land cover use by strata in the summer seasons, averaged over all years. For each stratum, three or four land covers tend to be dominantly used.

Name	Spatial Resolution	Year Origin	Source
Land use	25m x 25m & 10m x 10m	2003 & 2018 (continuously updated)	The Swedish Environmental Protection Agency, simplified into 7 classes.
Elevation	50m x 50m	2015	Lantmäteriet
Terrain Ruggedness Index (Riley et al., 1999)	50m x 50m	2015	Derived from DEM (Lantmäteriet)
Distance to Water	25m x 25 m	2003	Derived from land use (using proximity raster distance in QGIS).

Table 1: Geographical covariates used within the step selection analysis

3.3 Sampling Local Weather Through Space-Time Regression Kriging

To assess the effects of temperature extremes at fine spatial scales, several options for obtaining temperature data were considered: collar-derived sensors, the nearest weather station, and spatial interpolation methods. Collar-derived temperature data were ultimately rejected, as these sensors can produce outliers due to influences such as solar radiation, body heat, and wind exposure, limiting their interpretability for fine-scale environmental analysis. Although the use of the nearest weather station was also evaluated, this method was deemed inadequate for alpine and mountainous areas, where temperature varies strongly with elevation and local topography. As a result, space-time regression kriging was selected as the most suitable interpolation method. This approach allows for the incorporation of key predictors such as elevation, latitude, and day of the year, improving the representation of local temperature patterns over both space and time.

Data Collection and Regression Modeling

Weather data were obtained from the Swedish Meteorological and Hydrological Institute (SMHI) via their publicly available API. A Python package was developed to request and store weather data automatically in a PostgreSQL database (Appendix 2). Only weather stations with a "good" (G) quality rating, as indicated by the SMHI API, were included. Furthermore, to minimize spatial redundancy, stations located within 100 meters of another station were removed. Space-time regression kriging was implemented in R using the gstat and spacetime packages, following the methodology described by Sekulić et al. (2020). The first step involved fitting a regression model to the weather station data collected across all summer seasons within the study period. Explanatory variables included the year of measurement, a second-degree orthogonal polynomial of elevation, and the Geometric Temperature Trend (GTT), a variable that predicts daily mean temperature based on latitude and day of the year (Kilibarda et al. 2014). This regression model captured the broad spatial and temporal trends in temperature before kriging was applied to model the local residual variation.

Kriging Procedure

Following regression, space-time kriging was performed on the residuals to capture localized deviations from the large-scale temperature trend. Given the large volume of temperature observations, it was not computationally feasible to generate a single experimental semi-variogram for all available data. Space-time kriging is computationally intensive, with cubic time complexity, meaning that a tenfold increase in data points leads to a thousandfold increase in computation time (Yang et al. 2022). To balance computational feasibility with the need to capture short-term temperature variability, kriging was performed on a weekly basis. Weekly aggregation allowed the model to remain sensitive to short-term fluctuations, such as heatwaves, while ensuring that computational load remained manageable. Empirical and theoretical variograms were fitted separately for each week based on the residuals of the regression model. A small nugget effect was included to mitigate the screening effect, as some weather stations remained relatively close even after the filtering step (Stein 2002). Kriging was performed directly at the moose localization points rather than across a general prediction grid, targeting the specific locations of interest. Kriging computations were parallelized using the parabar package and conducted on a virtual machine hosted on DigitalOcean, with 48 CPU cores allocated. The full interpolation process required approximately 24 hours to complete. No unrealistic temperature artifacts were observed in the kriging outputs.

Model Validation

Model performance was evaluated using K-fold cross-validation. For each week, the weather station data were randomly divided into five folds, creating distinct training and validation sets. This procedure allowed the model to be tested across both spatial and temporal dimensions, offering a more thorough validation than methods based solely on spatial holdout, such as omitting entire stations. Although SMHI stations varied in their sampling frequency (with some recording hourly and others every three hours), the absence of significant temporal gaps in the data made K-fold cross-validation appropriate. A summary of the regression model and kriging validation results is provided in the Results section, while full details are presented in Appendix 1.

3.4 Step Selection Functions

For each stratum, a Step Selection Function (SSF) model was created to investigate habitat selection by moose. Two separate models were fitted: one based on localizations that occurred during heatwaves and one based on localizations outside of heatwaves. Heatwaves were defined using biological extremes rather than climatological thresholds, as the precise onset of heat stress in moose remains debated [expand on this and provide the sources for the captive moose study]. Specifically, a heatwave was defined as a period of three or more consecutive days in which the daily maximum temperature exceeded the 80th percentile of the available moose temperature data within each stratum.

Model Covariates

Movement-related variables were included to account for the underlying movement process and to construct an integrated step selection function . These consisted of step length, its logarithm, and turning angle. Environmental variables were included at the end of each step and consisted of land use, distance to the nearest water body, and elevation. Each of the environmental covariates was given an interaction with the temperature at the end of the step to investigate how habitat selection varied as a function of thermal conditions. End-step temperatures were used instead of start-step temperatures because GPS localizations occurred at relatively coarse temporal intervals of approximately three hours. With such intervals, substantial environmental changes can occur along the step trajectory, making the end-point conditions a better approximation of the microenvironment ultimately selected by the animal. This ensured that modeled selection reflected actual conditions at the chosen location rather than at the beginning of the movement path.

In addition to temperature interactions, harmonic terms were included to account for cyclical daily patterns. Two pairs of sine and cosine terms were used to model time-of-day effects, one pair for the start of the step and one for the end. Following formula 2.2 with $j = 1$ for one pair and $j = 2$ for the second pair. These were interacted with both environmental and movement variables to allow selection to vary over the course of the day. Following Signer et al. (2019) the movement terms were interacted with harmonic terms calculated at the start of each step to investigate how the animals current conditions influence movement. In contrast, interactions for habitat-related variables used harmonic terms at the end of the step, as the aim was to assess habitat selection based on the conditions in the area to which the animal moved (i.e. selected for).

Tertiary interactions among environmental variables, time of day, and temperature were not included, as heatwave and non-heatwave conditions were already analyzed separately through distinct models. All variables were tested for collinearity using the Generalized Variance Inflation Factor (GVIF), adjusted for degrees of freedom, with GVIF being < 2 for all variables.

Model Fitting

Models were fitted using a two-step approach. First, an SSF was fitted separately for each individual moose, without random effects. Second, population-level inference was obtained by aggregating individual coefficients through an intercept-only linear regression (eq. 8). Each coefficient was weighted by the inverse of its variance as per the two-stage procedure of fitting population level SSF (Fieberg et al. 2010; Muff et al. 2020)

$$fit = lm(coef \sim 1, weights = inv\_var) \tag{8}$$

The SSF model formula used for individual-level fits is given in formula 9

$$
\begin{gathered}
\text{case} \sim \\
\underbrace{\text{landuse\_end} + \text{dist\_to\_water\_end} + \text{elevation\_end}}_{\text{Main habitat terms}} + \\
\underbrace{\text{ruggedness\_end}}_{\text{Terrain cost term}} + \\
\underbrace{\text{sl} + \log(\text{sl}) + \cos(\text{ta})}_{\text{Movement terms}} + \\
\underbrace{\begin{matrix}(\text{landuse\_end} + \text{dist\_to\_water\_end} + \text{elevation\_end}): \\ (\text{hour\_s1\_t2} + \text{hour\_c1\_t2} + \text{hour\_s2\_t2} + \text{hour\_c2\_t2})\end{matrix}}_{\text{Habitat} \times \text{time interactions}} + \\
\underbrace{\begin{matrix}(\text{sl} + \log(\text{sl}) + \cos(\text{ta})): \\ (\text{hour\_s1\_t1} + \text{hour\_c1\_t1} + \text{hour\_s2\_t1} + \text{hour\_c2\_t1})\end{matrix}}_{\text{Movement} \times \text{time interactions}} + \\
\underbrace{\text{strata(step\_id)}}_{\text{Stratified matched design}}
\end{gathered} \tag{9}
$$

Equation 9: Model used for integrated step selection analysis. Habitat selection and movement were modeled using main effects (e.g. land use, elevation), movement terms (step length, log-transformed step length, and cosine of turning angle), and interactions with time of day (harmonic terms). Harmonic terms were constructed using sine and cosine transformations of the time of day at both the start (*_t1) and end (*_t2) of each step. Terms of the form hour_s1_t2, hour_c2_t1, etc., represent sinusoidal transformations with 2 cycles per 24 hours, enabling the model to capture diel activity rhythms and their influence on both movement and habitat selection.

4. Results

4.1 Heatwave events

The Boreal Alpine stratum experienced the greatest number of heatwave days (n = 220), followed by the Boreal Inland (n = 147) and Boreal Coast (n = 141), and Temperate (n = 59) strata (Figure 4). The number of GPS localizations available for analysis during heatwave and control conditions varied among strata (Table 2).

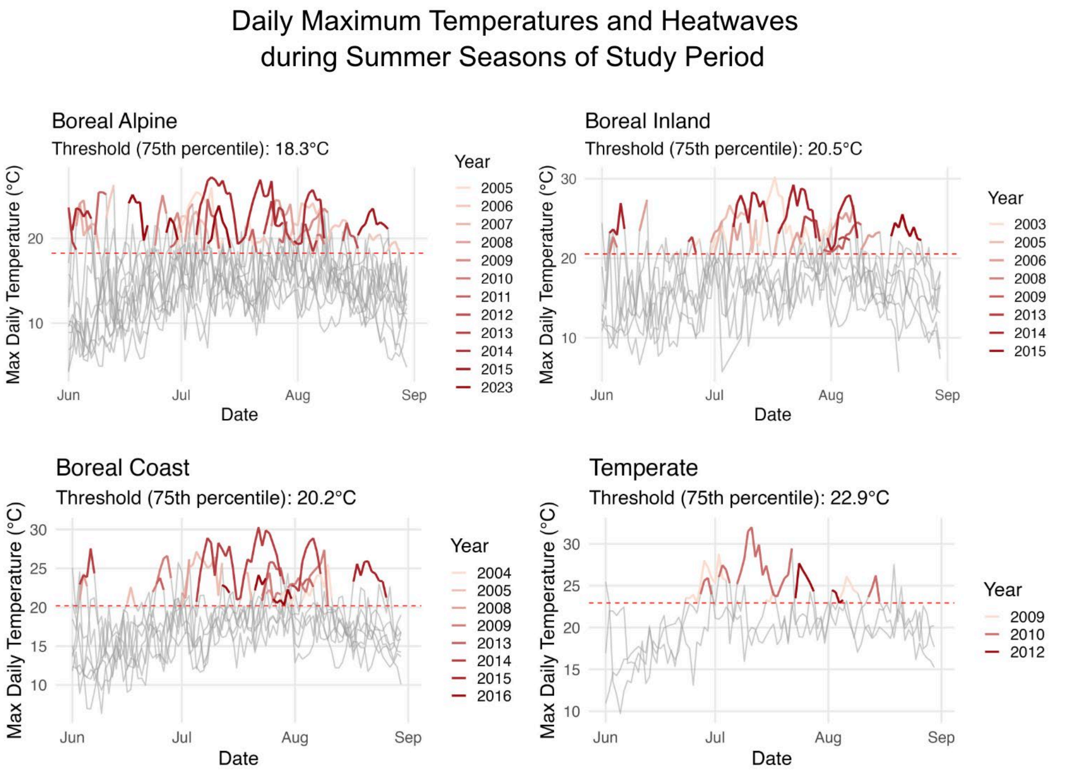

Figure 4: Daily maximum temperature throughout the study period for each climatic stratum. Heatwave periods, defined as three or more consecutive days above the 75th percentile of maximum temperature, are highlighted in red. Separate panels show data from the Boreal Alpine, Boreal Inland, Boreal Coastal, and Temperate regions, illustrating spatiotemporal variation in temperature, frequency and timing of extreme heat events.

	Boreal Alpine	Boreal Inland	Boreal Coast	Temperate
Control Dataset	102585	18052	40457	59347
Heatwave Dataset	31237	6881	9660	13667

Table 2: Number of GPS locations recorded in each bioclimatic region for control and heatwave datasets.

4.2 Movement during heatwave events

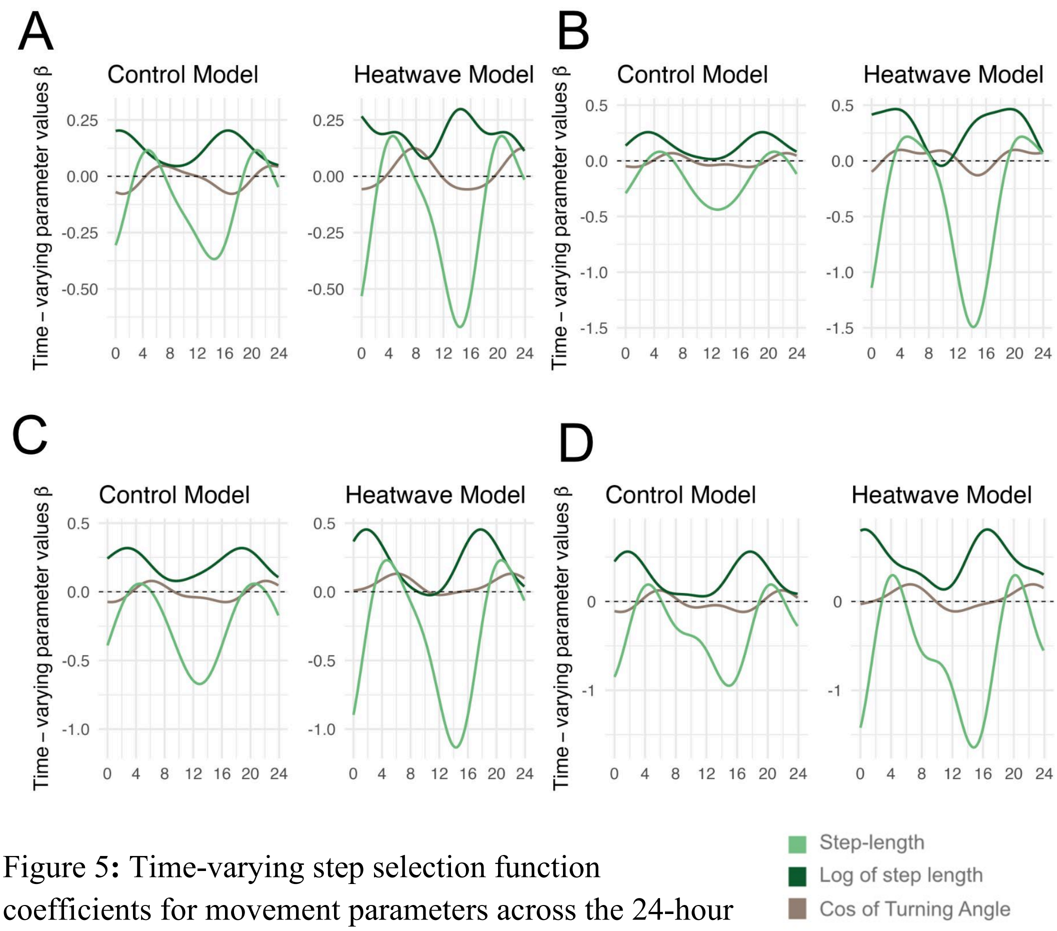

Figure 5**:** Time-varying step selection function coefficients for movement parameters across the 24-hour cycle. Colored lines show the effect of turning angle, log-transformed step length, and step length on step selection across hours of the day. Panel A: Boreal alpine, Panel B: Boreal inland, Panel C: Boreal coastal, Panel D: Temperate.

Time-varying coefficients for step length, log-transformed step length, and turning angle revealed distinct circadian patterns across strata (Figure 5). Across all regions, selection for longer step lengths sharply decreased around solar noon during heatwave events. In all but the temperatre strata, during nighttime hours in heatwaves the selection for longer steps slightly increased.

4.3 Landuse preference during heatwave events

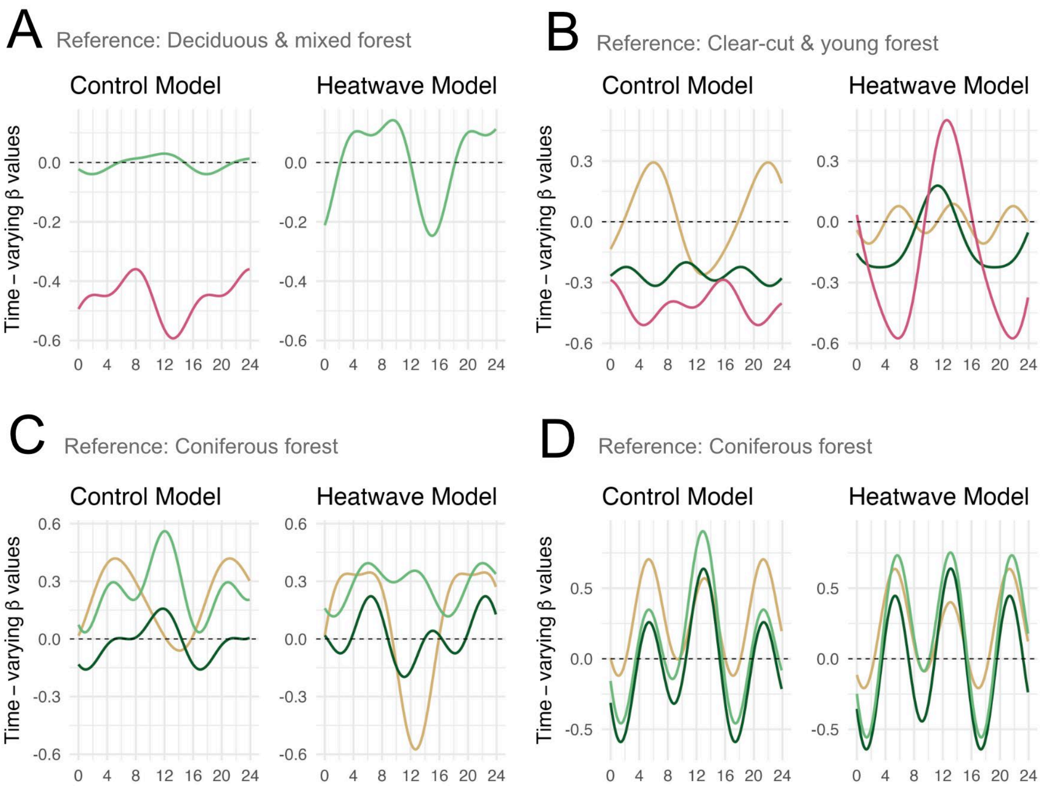

Figure 6: Time-varying habitat selection coefficients across four climate strata under control and heatwave conditions. Lines represent selection relative to the reference habitat indicated in each panel, showing how moose adjusted habitat use across the 24-hour cycle. Panel A: Boreal alpine, Panel B: Boreal inland, Panel C: Boreal coastal, Panel D: Temperate.

Circadian patterns of habitat selection varied across climate strata and differed between control and heatwave conditions (Figure 6). In all models, habitat selection was modeled relative to a baseline habitat type, typically the most commonly visited habitat within each stratum. Coefficients represent the time-varying strength and direction of selection throughout the 24-hour cycle.

In the boreal alpine stratum, moose exhibited a modest increase in selection for deciduous and mixed forests around midday during heatwave events. Wetland selection coefficients could not be estimated under heatwave conditions due to low visitation rates. In the boreal inland stratum, moose showed pronounced circadian rhythms in selection of clear-cut forests under control conditions. Clear-cut and young forests were strongly selected during nocturnal and early morning hours, while coniferous forest and wetlands were consistently avoided. Under heatwave conditions selection for clear-cuts diminished, and both coniferous forest and wetland habitats exhibited a peak in selection around the time of solar noon. In the Boreal Coastal region, a similar circadian rhythm of clear-cut and young forest is observed, but dedicious forest is also generally selected for relative to coniferous forest. During heatwave conditions selection persists, however avoidance of clear-cut and young forests starts to occur around the time of solar noon. In the temperate stratum, an odd trimodal selection pattern was observed, where all categories appear to have the same selection, which peaks during the crepescular periods and solar noon. Patterns appear stable between control and heatwave conditions.

4.4 Elevation and distance to water preference during heatwave events

Patterns of selection for elevation and distance to water varied across strata but revealed consistent patterns (Figure 7). Across all climate strata, moose selected locations at lower than mean elevations, particularly around midday. This downward movement peaked during the warmest parts of the day and was amplified under heatwave conditions. In the boreal alpine stratum, moose showed positive selection for distance to water during daylight hours, meaning they tended to move away from water bodies during the day. This pattern was observed only in the boreal alpine stratum and boreal coast stratum during heatwaves, with no clear daytime avoidance of water seen in the other strata.

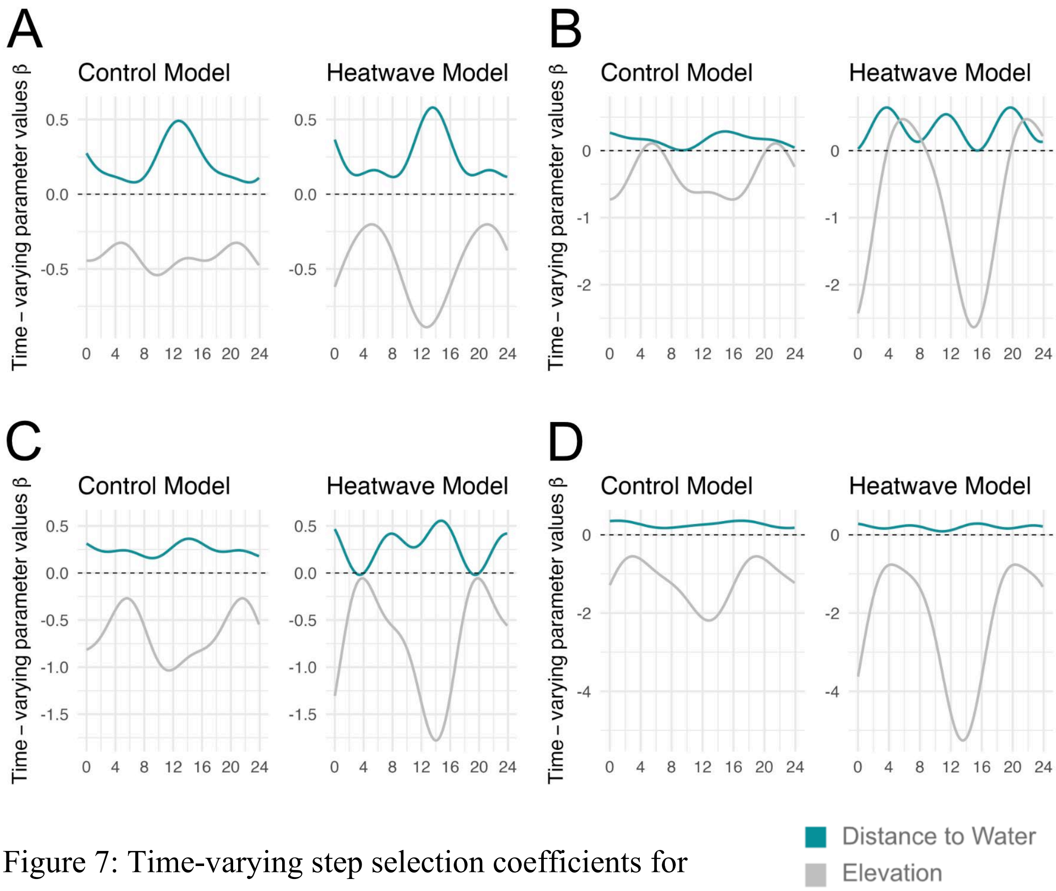

Figure 7: Time-varying step selection coefficients for elevation and distance to water across all four strata. Lines represent selection across the 24-hour cycle, with separate curves shown for control and heatwave models. Positive values indicate selection for greater elevation or distance to water relative to the standardized mean of these variables. Panel A: Boreal alpine, Panel B: Boreal inland, Panel C: Boreal coastal, Panel D: Temperate.

5. Discussion and Conclusion

This study examined how Swedish moose respond to heatwave events during summer (Jun-Aug) using fine-scale movement and habitat data across varying ecological contexts. The results provide both support and nuance for the hypotheses posed, particularly in the context of behavioral thermoregulation, diel rhythmicity, and spatial habitat use.

Heat-Avoidance Behavior Hypothesis

Moose adjusted their behavior during heatwaves, reducing movement during the hottest hours of the day and slightly increasing activity at night, supporting my hypothesis that moose will adjust their movement behavior in relation to ambient temperatures. This aligns with prior observations that moose typically reduce daytime movement in response to heat stress and mirrors patterns of nocturnal compensation observed in other cold-adapted ungulates under warming conditions (Jennewein et al. 2020; Brivio et al. 2024). In addition to movement patterns, habitat selection during heatwaves was affected in some strata. In the boreal inland strata, moose selected for forest over clear-cut and young forest in the middle of the day during heatwaves, consistent with their use as thermal refuge. Although such increased selection did not occur in the boreal coast strata, a decrease in selection for clear-cut and young forest was found. These behavioral adjustments are consistent with a thermoregulatory strategy in which moose trade foraging or exploration during daytime for thermal comfort in shaded microclimates, thereby affirming the presence of active heat-avoidance strategies. I did not see evidence of thermoregulatory behaviour in moose in the temporal region, though limitations to this strata apply which will be further explain below.

Circadian Rhythm Modulation Hypothesis

Moose exhibited seasonal variation in movement across all strata, regardless of latitude or the occurrence of heatwaves. The heatwave model provided evidence that circadian rhythms were influenced by temperature, with movement showing stronger seasonal patterns. In the boreal strata, where the day-night cycle is absent during summer, these findings underscore the importance of analyzing circadian rhythms using cues other than light. This is particularly relevant when behavioral responses across the full 24-hour cycle are difficult to assess due to the continuous daylight of the polar summer. Although previous studies have reported diminished circadian rhythms in boreal ungulates such as moose (Græsli et al. 2020) and reindeer (van Oort et al. 2007), the present study found a strong circadian rhythm. This aligns with alternative findings from Svalbard reindeer, which also maintain robust circadian patterns despite the absence of a conventional light-dark cycle (Arnold et al. 2018).

Foraging Opportunity Hypothesis

My findings have limited support to the expectation that moose would offset reduced daytime foraging by selectively using high-quality foraging habitats, such as clear-cuts or young forest stands, during cooler twilight periods. However, this pattern was not consistently observed across strata. Although moose did increase movement slightly during evening and early morning hours, there was little consistent evidence of elevated selection for the preferred foraging habitat of clear-cut and young forest during those windows. This suggests either that thermal priorities override foraging priorities under extreme heat, or that the available land cover data were insufficiently detailed to detect such selection.

Water-Seeking Behavior Hypothesis

Although previous studies have reported increased use of wetlands and riparian areas by moose during hot periods (Jennewein et al. 2020), the present analysis did not meet the prediction of closer proximity to water during heatwaves. This suggests that water did not play a central role in habitat selection during heatwaves in the study system. In fact, moose tended to increase their distance from water during the hottest parts of the day, with little difference between control and heatwave days. One plausible explanation is the resolution of the spatial data: water availability was primarily defined by large rivers and lakes, potentially overlooking smaller aquatic features that may serve as thermal refuges. Without fine-scale hydrological data, it remains difficult to fully assess water-seeking behavior during heat events.

Regarding wetlands, moose in boreal alpine regions appeared to avoid these features under heat stress, as there were few observations of wetland use during heatwaves despite a large sample size. Notably, clear selection for wetlands occurred in boreal inland strata, where strong selection was observed around noon during heatwaves, but not on control days.

Topographic Refuge Hypothesis

Findings related to the Topographic Refuge Hypothesis were unexpected. While the hypothesis predicted that moose in alpine regions would ascend to higher elevations during heatwaves to access cooler temperatures, the analysis showed the opposite: moose consistently selected lower elevations at midday, with this tendency becoming more pronounced as temperatures increased. This pattern was consistent across all strata. In the alpine region, lower elevations often supported denser forest cover and more productive vegetation, which may partly explain the observed selection. Additionally, the hypothesis did not account for the energetic costs and heat production associated with uphill movement, which could further discourage ascent during periods of thermal stress.

Limitations

The 3-hour fix rate of GPS collars may miss short-term adjustments. The harmonic modeling framework used was constrained to two harmonic terms due to convergence issues, which may have limited the resolution of diel variability. Coarse habitat classification and lack of canopy-specific metrics may have further limited detection of habitat specificity. Additionally, modeling constraints, such as requiring moose to encounter each habitat type at each time point, reduced the sample size available for interaction effects. Habitat availability was also not incorporated into the selection, which means that currently all habitats are considered equally available. Future work considering categorical habitat data should apply a weight to the habitat coefficients relative to their abundance.

I attempted at finding statistically significant changes in selection when carrying out the time-varying step selection functions. For this I incorporated an empirical bootstrap of the step selection function coefficients. However, when deriving the confidence intervals for the harmonic interaction terms, phase shifts in the circadian pattern between bootstrap replicates introduced challenges. Changing the coefficient for a cosine or sine term shifts the wave to the left or right. This resulted in confidence intervals where lower and upper bounds for coefficients can swap, as the coefficients are cyclical. My limited experience with harmonic regression means I did not attempt to interpretate this or explore this further, but future work should focus on this limitation. These constraints suggest caution in interpreting the exact magnitude of observed effects. Alternatively, recent studies have employed splines or hierarchical random effect models that do not encounter this issue, at the cost of computational time-complexity (Klappstein et al. 2024).

Conclusion

This study provides nuanced insight into how Swedish moose respond to extreme summer heat across ecological contexts, revealing support for behavioral thermoregulation through reduced daytime movement and increased use of shaded habitats. Although some hypotheses, such as the heat-avoidance behavior and circadian rhythm modulation, were supported, others, like water-seeking, foraging compensation, and topographic refuge, received limited or contradictory support. These findings highlight the complexity of moose responses to thermal stress and underscore the need for high-resolution environmental data to detect fine-scale behavioral strategies.

Recommendations

This study highlights several areas for improvement in future research. First, the use of three pairs of harmonics for modeling diel patterns resulted in convergence issues, as some animals did not visit all habitat types at every harmonic timestamp. This led to missing interaction terms, making two pairs the most reliable option. Future work should explore alternative methods, such as optimizing harmonic regression frameworks or employing higher GPS fix rates, to improve model stability and ensure all interaction terms are captured (Forrest et al. 2025).

Regarding spatial resolution, the quality of the landcover maps used in this study was limited. While an attempt was made to work with available data, future studies should incorporate more detailed remote sensing-derived indices, such as NDVI (Normalized Difference Vegetation Index), to better capture habitat characteristics that are crucial for understanding moose behavior (Verzuh et al. 2023b). Additionally, high-resolution LiDAR or satellite-based vegetation structure data would provide a more accurate representation of habitat features, improving the ability to detect subtle behavioral patterns in response to heat stress (Melin et al. 2014).

The bootstrapping method used for calculating confidence intervals was challenged by phase shifts, particularly when deriving harmonic term interaction effects. To address this, alternative methods like splines or hierarchical random effect models could better accommodate cyclical data and improve the accuracy of confidence intervals (Klappstein et al. 2024). These models would allow for better resolution of temporal dynamics.

Finally, future studies should consider anchoring time by daylight length when analyzing circadian rhythms, particularly in high-latitude regions with significant variation in daylight duration (Vazquez et al. 2019). Adjusting for daylight length would improve the accuracy of behavioral models across different seasons and better account for the influence of photoperiod on moose activity patterns.

Incorporating these improvements will help refine our understanding of moose behavior in response to extreme weather events and provide more robust data for wildlife management in a changing climate.

References

Arnold, W., Ruf, T., Loe, L.E., Irvine, R.J., Ropstad, E., Veiberg, V. & Albon, S.D. (2018). Circadian rhythmicity persists through the Polar night and midnight sun in Svalbard reindeer. *Scientific Reports*, 8 (1), 14466. https://doi.org/10.1038/s41598-018-32778-4

van Beest, F.M. & Milner, J.M. (2013). Behavioural responses to thermal conditions affect seasonal mass change in a heat-sensitive northern ungulate. *PloS One*, 8 (6), e65972. https://doi.org/10.1371/journal.pone.0065972

van Beest, F.M., Van Moorter, B. & Milner, J.M. (2012). Temperature-mediated habitat use and selection by a heat-sensitive northern ungulate. *Animal Behaviour*, 84 (3), 723–735. https://doi.org/10.1016/j.anbehav.2012.06.032

Beltran, R.S. & Tarwater, C.E. (2024). Overcoming the pitfalls of categorizing continuous variables in ecology, evolution and behaviour. *Proceedings of the Royal Society B: Biological Sciences*, 291 (2032), 20241640. https://doi.org/10.1098/rspb.2024.1640

Brivio, F., Apollonio, M., Anderwald, P., Filli, F., Bassano, B., Bertolucci, C. & Grignolio, S. (2024). Seeking temporal refugia to heat stress: increasing nocturnal activity despite predation risk. *Proceedings of the Royal Society B: Biological Sciences*, 291 (2015). https://doi.org/10.1098/rspb.2023.1587

Bump, J.K., Bergman, B.G., Schrank, A.J., Marcarelli, A.M., Kane, E.S., Risch, A.C. & Schütz, M. (2017). Nutrient release from moose bioturbation in aquatic ecosystems. *Oikos*, 126 (3), 389–397. https://doi.org/10.1111/oik.03591

Chatterjee, N., Wolfson, D., Kim, D., Velez, J., Freeman, S., Bacheler, N.M., Shertzer, K., Taylor, J.C. & Fieberg, J. (2024). Modelling individual variability in habitat selection and movement using integrated step-selection analysis. *Methods in Ecology and Evolution*, 15 (6), 1034–1047. https://doi.org/10.1111/2041-210X.14321

Cressie, N.A.C. & Wikle, C.K. (2011). *Statistics for spatio-temporal data*. Wiley. (Wiley series in probability and statistics)

Dettki, H., Ericcson, G., Giles, T. & Norrsken-Ericsson, M. (2013). Wireless Remote Animal Monitoring (WRAM) - A new international database e-infrastructure for telemetry sensor data from fish and wildlife. In: *Proceedings Etc. 2012: Convention for Telemetry, Test Instrumentation and Telecontrol*. The European Society of Telemetry. 247–256.

Felton, A.M., Wam, H.K., Borowski, Z., Granhus, A., Juvany, L., Matala, J., Melin, M., Wallgren, M. & Mårell, A. (2024). Climate change and deer in boreal and temperate regions: From physiology to population dynamics and species distributions. *Global Change Biology*, 30 (9), e17505. https://doi.org/10.1111/gcb.17505

Fieberg, J., Matthiopoulos, J., Hebblewhite, M., Boyce, M.S. & Frair, J.L. (2010). Correlation and studies of habitat selection: problem, red herring or opportunity? *Philosophical Transactions of the Royal Society B: Biological Sciences*, 365 (1550), 2233–2244. https://doi.org/10.1098/rstb.2010.0079

Fieberg, J., Signer, J., Smith, B. & Avgar, T. (2021). A 'How to' guide for interpreting parameters in habitat-selection analyses. *Journal of Animal Ecology*, 90 (5), 1027–1043. https://doi.org/10.1111/1365-2656.13441

Forrest, S.W., Pagendam, D., Bode, M., Drovandi, C., Potts, J.R., Perry, J., Vanderduys, E. & Hoskins, A.J. (2025). Predicting fine-scale distributions and emergent spatiotemporal patterns from temporally dynamic step selection simulations. *Ecography*, 2025 (2), e07421. https://doi.org/10.1111/ecog.07421

Græsli, A.R., Thiel, A., Fuchs, B., Singh, N.J., Stenbacka, F., Ericsson, G., Neumann, W., Arnemo, J.M. & Evans, A.L. (2020). Seasonal Hypometabolism in Female Moose. *Frontiers in Ecology and Evolution*, 8. https://www.frontiersin.org/articles/10.3389/fevo.2020.00107 [2024-01-17]

Hengl, T., Heuvelink, G.B.M. & Rossiter, D.G. (2007). About regression-kriging: From equations to case studies. *Computers & Geosciences*, 33 (10), 1301–1315. https://doi.org/10.1016/j.cageo.2007.05.001

Hetem, R.S., Fuller ,Andrea, Maloney ,Shane K & and Mitchell, D. (2014). Responses of large mammals to climate change. *Temperature*, 1 (2), 115–127. https://doi.org/10.4161/temp.29651

Jennewein, J.S., Hebblewhite, M., Mahoney, P., Gilbert, S., Meddens, A.J.H., Boelman, N.T., Joly, K., Jones, K., Kellie, K.A., Brainerd, S., Vierling, L.A. & Eitel, J.U.H. (2020). Behavioral modifications by a large-northern herbivore to mitigate warming conditions. *Movement Ecology*, 8 (1), 39. https://doi.org/10.1186/s40462-020-00223-9

Kilibarda, M., Hengl, T., Heuvelink, G.B.M., Gräler, B., Pebesma, E., Perčec Tadić, M. & Bajat, B. (2014). Spatio-temporal interpolation of daily temperatures for global land areas at 1 km resolution. *Journal of Geophysical Research: Atmospheres*, 119 (5), 2294–2313. https://doi.org/10.1002/2013JD020803

Klappstein, N.J., Michelot, T., Fieberg, J., Pedersen, E.J. & Mills Flemming, J. (2024). Step selection functions with non-linear and random effects. *Methods in Ecology and Evolution*, 15 (8), 1332–1346. https://doi.org/10.1111/2041-210X.14367

Langrock, W.Z., Iain L. MacDonald, Roland (2016). *Hidden Markov Models for Time Series: An Introduction Using R, Second Edition*. 2. ed. Chapman and Hall/CRC. https://doi.org/10.1201/b20790

Lantmateriet (2009). Swedish Digital Elevation Model. www.lantmateriet.se

Lenarz, M.S., Nelson, M.E., Schrage, M.W. & Edwards, A.J. (2009). Temperature Mediated Moose Survival in Northeastern Minnesota. *The Journal of Wildlife Management*, 73 (4), 503–510. https://doi.org/10.2193/2008-265

Mawer, R., Bruneel, S.P., Pauwels, I.S., Elings, J., Pickholtz, E., Pickholtz, R., Schneider, M., Coeck, J. & Goethals, P.L.M. (2023). Individual variation in the habitat selection of upstream migrating fish near a barrier. *Movement Ecology*, 11 (1), 49. https://doi.org/10.1186/s40462-023-00414-0

McCann, N.P., Moen, R.A. & Harris, T.R. (2013). Warm-season heat stress in moose (*Alcesalces*). *Canadian Journal of Zoology*, 91 (12), 893–898. https://doi.org/10.1139/cjz-2013-0175

McClintock, B.T. & Michelot, T. (2018). momentuHMM: R package for generalized hidden Markov models of animal movement. *Methods in Ecology and Evolution*, 9 (6), 1518–1530. https://doi.org/10.1111/2041-210X.12995

Melin, M., Matala, J., Mehtätalo, L., Tiilikainen, R., Tikkanen, O.-P., Maltamo, M., Pusenius, J. & Packalen, P. (2014). Moose (Alces alces) reacts to high summer temperatures by utilizing thermal shelters in boreal forests - an analysis based on airborne laser scanning of the canopy structure at moose locations. *Global Change Biology*, 20 (4), 1115–1125. https://doi.org/10.1111/gcb.12405

Messeri, A., Becciolini, V., Messeri, G., Morabito, M., Crisci, A., Orlandini, S. & Ponzetta, M.P. (2019). Wild ungulates and environmental temperature: analysis on the possible utilization of data from sensor placed on GPS collars. *International Journal of Biometeorology*, 63 (3), 293–300. https://doi.org/10.1007/s00484-018-01662-1

Monteith, K.L., Klaver, R.W., Hersey, K.R., Holland, A.A., Thomas, T.P. & Kauffman, M.J. (2015). Effects of climate and plant phenology on recruitment of moose at the southern extent of their range. *Oecologia*, 178 (4), 1137–1148. https://doi.org/10.1007/s00442-015-3296-4

Montero, J.-M., Fernández-Avilés, G. & Mateu, J. (2015). *Spatial and Spatio-Temporal Geostatistical Modeling and Kriging*. John Wiley & Sons.

Montgomery, R.A., Redilla, K.M., Moll, R.J., Van Moorter, B., Rolandsen, C.M., Millspaugh, J.J. & Solberg, E.J. (2019). Movement modeling reveals the complex nature of the response of moose to ambient temperatures during summer. *Journal of Mammalogy*, 100 (1), 169–177. https://doi.org/10.1093/jmammal/gyy185

Muff, S., Signer, J. & Fieberg, J. (2020). Accounting for individual-specific variation in habitat-selection studies: Efficient estimation of mixed-effects models using Bayesian or frequentist computation. *Journal of Animal Ecology*, 89 (1), 80–92. https://doi.org/10.1111/1365-2656.13087

Naturvårdsverket (2003). Nationella marktäckedata. https://www.naturvardsverket.se/verktyg-och-tjanster/kartor-och-karttjanster/nationella-marktackedata/

Neumann, W., Ericsson, G., Dettki, H., Bunnefeld, N., Keuler, N.S., Helmers, D.P. & Radeloff, V.C. (2012). Difference in spatiotemporal patterns of wildlife road-crossings and wildlife-vehicle collisions. *Biological Conservation*, 145 (1), 70–78. https://doi.org/10.1016/j.biocon.2011.10.011

Niedziałkowska, M., Neumann, W., Borowik, T., Kołodziej-Sobocińska, M., Malmsten, J., Arnemo, J.M. & Ericsson, G. (2022). Moose Alces alces (Linnaeus, 1758). In: Hackländer, K. & Zachos, F.E. (eds) *Handbook of the Mammals of Europe*. Springer International Publishing. 1–32. https://doi.org/10.1007/978-3-319-65038-8_23-1

van Oort, B.E.H., Tyler, N.J.C., Gerkema, M.P., Folkow, L., Blix, A.S. & Stokkan, K.-A. (2005). Circadian organization in reindeer. *Nature*, 438 (7071), 1095–1096. https://doi.org/10.1038/4381095a

van Oort, B.E.H., Tyler, N.J.C., Gerkema, M.P., Folkow, L. & Stokkan, K.-A. (2007). Where clocks are redundant: weak circadian mechanisms in reindeer living under polar photic conditions. *Naturwissenschaften*, 94 (3), 183–194. https://doi.org/10.1007/s00114-006-0174-2

Persson, I.-L., Danell, K. & Bergström, R. (2005). Different Moose Densities and Accompanied Changes in Tree Morphology and Browse Production. *Ecological Applications*, 15 (4), 1296–1305. https://doi.org/10.1890/04-0499

Renecker, L.A. & Hudson, R.J. (1989). Seasonal Activity Budgets of Moose in Aspen-Dominated Boreal Forests. *The Journal of Wildlife Management*, 53 (2), 296–302. https://doi.org/10.2307/3801126

Riley, S.J., DeGloria, S.D. & Elliot, R. (1999). Index that quantifies topographic heterogeneity. *intermountain Journal of sciences*, 5 (1–4), 23–27

Sekulić, A., Kilibarda, M., Protić, D., Tadić, M.P. & Bajat, B. (2020). Spatio-temporal regression kriging model of mean daily temperature for Croatia. *Theoretical and Applied Climatology*, 140 (1), 101–114. https://doi.org/10.1007/s00704-019-03077-3

Signer, J., Fieberg, J. & Avgar, T. (2019). Animal movement tools (amt): R package for managing tracking data and conducting habitat selection analyses. *Ecology and Evolution*, 9 (2), 880–890. https://doi.org/10.1002/ece3.4823

Stein, M.L. (2002). The screening effect in Kriging. *The Annals of Statistics*, 30 (1), 298–323. https://doi.org/10.1214/aos/1015362194

Stokkan, K.-A., Van Oort, B.E.H., Tyler, N.J.C. & Loudon, A.S.I. (2007). Adaptations for life in the Arctic: evidence that melatonin rhythms in reindeer are not driven by a circadian oscillator but remain acutely sensitive to environmental photoperiod. *Journal of Pineal Research*, 43 (3), 289–293. https://doi.org/10.1111/j.1600-079X.2007.00476.x

Swedish Forest Agency (Skogsstyrelsen) (2024). Digital Open Forest Data. https://www.skogsstyrelsen.se/en/digital-open-forest-data/

Thompson, D.P., Crouse, J.A., Jaques, S. & Barboza, P.S. (2020). Redefining physiological responses of moose (Alces alces) to warm environmental conditions. *Journal of Thermal Biology*, 90, 102581. https://doi.org/10.1016/j.jtherbio.2020.102581

Thurfjell, H., Ciuti, S. & Boyce, M.S. (2014). Applications of step-selection functions in ecology and conservation. *Movement Ecology*, 2 (1), 4. https://doi.org/10.1186/2051-3933-2-4

Van Moorter, B., Kivimäki, I., Panzacchi, M. & Saerens, M. (2021). Defining and quantifying effective connectivity of landscapes for species' movements. *Ecography*, 44 (6), 870–884. https://doi.org/10.1111/ecog.05351

Vazquez, C., Rowcliffe, J.M., Spoelstra, K. & Jansen, P.A. (2019). Comparing diel activity patterns of wildlife across latitudes and seasons: Time transformations using day length. *Methods in Ecology and Evolution*, 10 (12), 2057–2066. https://doi.org/10.1111/2041-210X.13290

Verzuh, T.L., Rogers, S.A., Mathewson, P.D., May, A., Porter, W.P., Class, C., Knox, L., Cufaude, T., Hall, L.E., Long, R.A. & Monteith, K.L. (2023a). Behavioural responses of a large, heat-sensitive mammal to climatic variation at multiple spatial scales. *Journal of Animal Ecology*, 92 (3), 619–634. https://doi.org/10.1111/1365-2656.13873

Verzuh, T.L., Rogers, S.A., Mathewson, P.D., May, A., Porter, W.P., Class, C., Knox, L., Cufaude, T., Hall, L.E., Long, R.A. & Monteith, K.L. (2023b). Behavioural responses of a large, heat-sensitive mammal to climatic variation at multiple spatial scales. *Journal of Animal Ecology*, 92 (3), 619–634. https://doi.org/10.1111/1365-2656.13873

Yang, Y., Wang, P. & Brandenberg, S.J. (2022). An algorithm for generating spatially correlated random fields using Cholesky decomposition and ordinary kriging. *Computers and Geotechnics*, 147, 104783. https://doi.org/10.1016/j.compgeo.2022.104783

Popular science summary

Moose are facing tough times as climate change brings more frequent and intense heatwaves to places like northern Sweden. This study looked closely at how hundreds of female moose, fitted with GPS collars, moved and chose their homes across different types of landscapes in Sweden. By carefully examining their tracking data and local weather information, the research aimed to figure out how moose change their behavior when it gets really hot. The findings show that moose have clever ways to deal with the heat. During heatwaves, they significantly cut down on their daytime movement, which is a key cooling strategy to save energy and avoid overheating. On top of that, moose changed where they preferred to be, often choosing denser forests and wetlands during the middle of the day. These areas act as important cool spots, offering shade and more humid conditions. Interestingly, in mountainous regions, moose were seen moving to lower elevations when it was hot, especially around noon. This might seem surprising, but lower areas often have more trees and richer plant life, which can provide better protection from the heat than exposed higher ground, and it also avoids the energy drain of moving uphill in the heat. On the other hand, the study didn't consistently find moose moving closer to big bodies of water during heatwaves. This could mean that other shaded spots are more important for cooling, or perhaps our data didn't capture smaller puddles or streams they might use. Despite the challenges of the heat and the long summer daylight in northern Sweden, moose largely stuck to their daily activity routines, showing they have a strong internal body clock. This research is important because moose are vital animals whose eating habits shape the forests and affect how the whole ecosystem works. Understanding how they'll cope in a warming world is essential for predicting their future and guiding how we manage wildlife, ultimately highlighting the need for diverse landscapes that offer them vital places to cool down.

Appendix 1 – Sampling Temperature with Space-Time Regression Kriging

SMHI Mock Database

To efficiently handle large volumes of weather data, I implemented a database layer between the client and the SMHI API. This layer minimizes redundant API requests and allows for faster querying during analysis. The backend is powered by PostgreSQL 16, extended with PostGIS to manage spatial vector data. PostgreSQL was chosen for its performance, scalability, and strong support for spatial operations. Data ingestion and querying were handled using Python. I used the requests library to communicate with the SMHI API, and SQLAlchemy to interface with the PostgreSQL database. This setup allowed me to seed the database with all available SMHI stations once, thereby eliminating the need for repeated API calls during subsequent analyses. Most weather stations in the database recorded temperature either hourly or every three hours. Three-hour intervals were more common in the earlier years of the study period, whereas hourly recordings became more frequent in later years.

Linear Regression Model

As the first step in the kriging workflow, I fitted a linear regression model using all available summer weather data from the study period (2004–2023). This model served to extract residuals that could be interpolated using kriging. The explanatory variables included elevation, the year of measurement, and Growing Temperature Threshold (GTT), which was calculated using the r-meteo package based on latitude and day of the year. The model accounted for 26.4 percent of the variation in temperature across the temporal window of interest. To assess whether a linear relationship was appropriate, I inspected a Q-Q plot of the residuals. The plot showed approximate normality, with only minor deviations at the higher end of the distribution. This indicated that the model's assumptions were reasonably satisfied. The coefficients of the regression model are shown in Table 1. Elevation had a small but consistent negative effect on temperature, while GTT showed a strong positive relationship. Yearly effects were significant across the entire range, except for the year 2022.

Variable name	B Estimate	Std.Error	P-value
(Intercept)	6.717	1.627e-02	<2e-16 ***
elevation	-5.533e-03	8.039e-06	<2e-16 ***
gtt	7.387e-01	8.507e-04	<2e-16 ***
Year 2004 till Year 2023	(,)	(,)	All <2e-16 ***

			except 2022 (0.593)

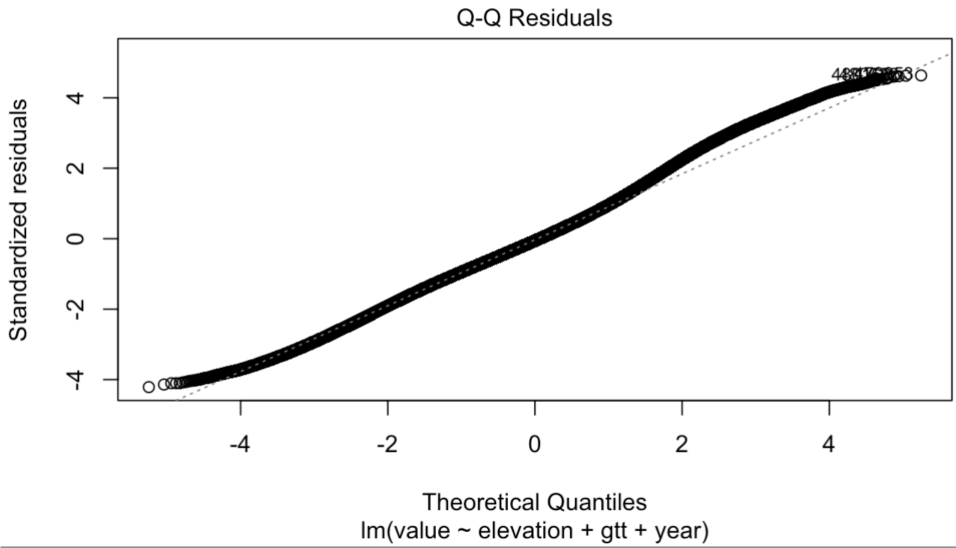

Semi-variogram Fitting

To address the computational demands of kriging, which has cubic time complexity, I divided the dataset into weekly intervals. This allowed me to run separate variogram models on each week, reducing memory and processing requirements. Across the different summer weeks I examined, I did not observe major differences in the fitted variograms. While this conclusion is based on visual inspection rather than formal testing, the same parameter values appeared to fit reasonably well throughout the summer period. This suggests that, although the underlying process may not be strictly stationary, the variogram model and parameters were consistently applicable to the data used. For illustration, I present the results for the week of 1 June to 7 June 2018. An empirical variogram was fitted using the spacetime package in R. I used this variogram to derive initial parameters for the model variogram (see Table 2). A small nugget effect was included for both the spatial and temporal dimensions. This decision was made to counteract the screening effect caused by the close proximity of some weather stations, which occasionally led to negative kriging weights. I then fitted a model variogram based on these initial values. The results of this fitted model are presented in Table 3.

	Partial-sill	Range	Nugget
Space	6	550000	0.001
Time	30	10	0
Joint	4	50000	0.001

	Partial-sill	Range	Nugget
Space	6.4286891	550000	0.3684194
Time	299.3258	193.5573	0
Joint	0.001	50000	0.001

I should be noted I did not perform a full sensitivity analysis to optimize starting values or parameter bounds. Instead, I selected a model that consistently converged and provided a good empirical fit. The sum-metric variogram model proved to be the most stable across different weeks and appeared well-suited to summer temperature data. For those planning to apply this methodology in other contexts, it is worth noting that I encountered more difficulty fitting variogram models to winter temperature data. In these cases, adjustments to the initial parameter values were often required to obtain a reasonable fit. While this was not central to my study, it may be an important consideration for future applications.

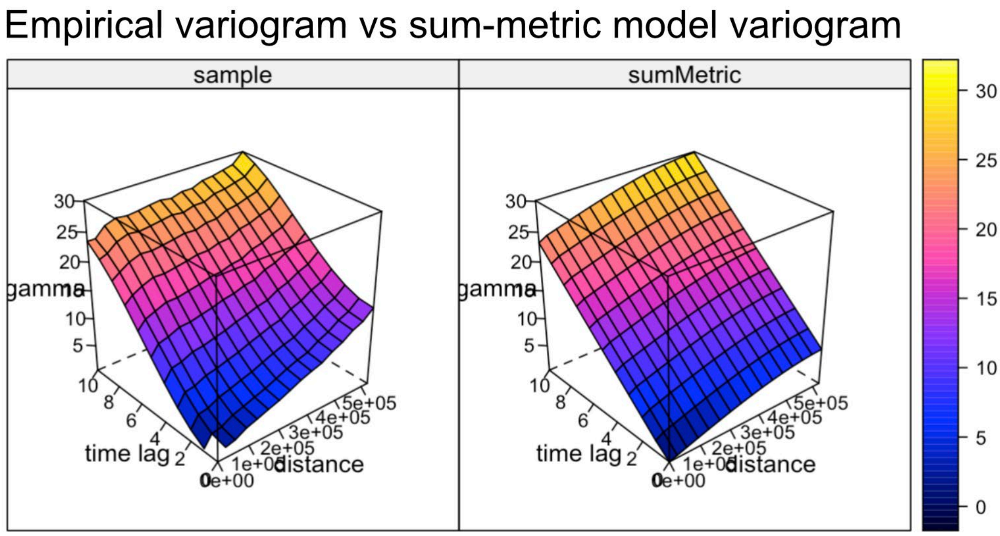

Cross Validation

To evaluate the accuracy of the space-time regression kriging model, I conducted a five-fold cross-validation. This involved dividing the weather dataset into five parts, training the model on four parts, and testing on the remaining one, cycling through all combinations. The model consistently explained approximately 96 percent of the variance in the held-out data across all folds. Mean absolute error was 0.96, and root mean square error was 1.36. These low error values indicate that the model has sufficient precision for the purposes of this study, where small deviations of a 1 or 2 degrees Celsius are unlikely to influence the overall results meaningfully.

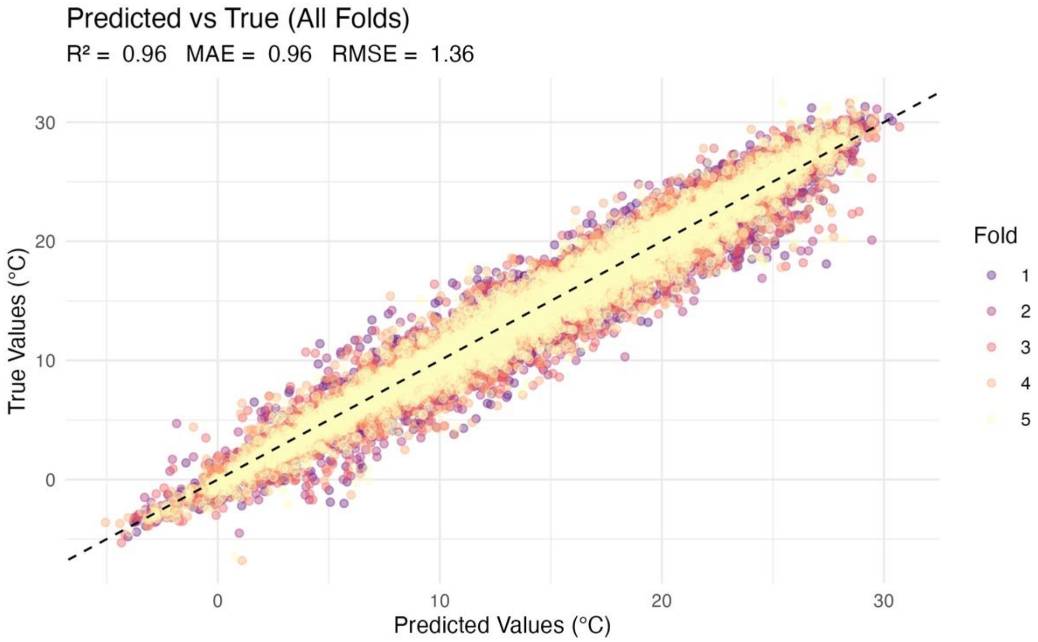

Predicitng Temperature at Moose Localisations

To estimate temperature at the locations of moose and random steps, I split the data into weekly batches. For each batch, I retrieved the corresponding week of weather data from the database, applied the linear regression model, fitted the variogram (using the same initial values as above), and then performed kriging. This was done independently for each batch, using the residuals from the regression as input for kriging. The entire process was parallelised using the parabar package.

Hardware Details

Parallellisation significantly reduced runtime for the most computationally expensive parts of the workflow. Annotating temperature at moose localisations using space-time regression kriging required approximately 20 hours using 48 CPU cores. This step was one of the most resource-intensive components of the entire analysis.

Appendix 2 – Code Availability

Quarto notebooks including explanations of the methodology and reproduction steps can be found at: https://github.com/Shmuppel/moose-temperature-ssf. View the README.md for help setting up the environment. All spatial data used foranalysis was kept in the coordinate reference system SWEREF-99 (EPSG:3006).

Publishing and archiving

☒ YES, I, Niels van der Vegt, have read and agree to the agreement for publication and the personal data processing that takes place in connection with this